Shaping apertures and masking

Erez N. Ribak and B. M. Levine

Department of Physics, Technion - Israel Institute of Technology
Haifa, Israel 32000

ABSTRACT

We propose to vary the shape of the sub-apertures both in cases of aperture masking and for segmented space telescopes. Most sub-apertures assume the shape of circles, rectangles and hexagons, but it is possible to use other shapes such as ellipses. Compared to polygons, ellipses reduce diffraction spokes in the PSF. They can have different axis ratios, and more importantly be placed at different rotation angles. This allows their easier identification in the focal plane for tip-tilt measurement. In the pupil auto-correlation (*uv*) plane it also allows the unique separation of sub-aperture pairs for piston measurements. Optimisation of separation angles lead to rough values of 67, 84, 113 and 96 degrees, for a range of ellipticity values.

Keywords: Aperture masking, sparse telescopes, space telescopes

1. **Introduction**

While surveying designs for a deployable space telescope with sparse segments and their alignment [1-8], we found that many designs use rectangular or hexagonal segments. These shapes are important for contiguous telescopes, since the continuous tiling uses better the back

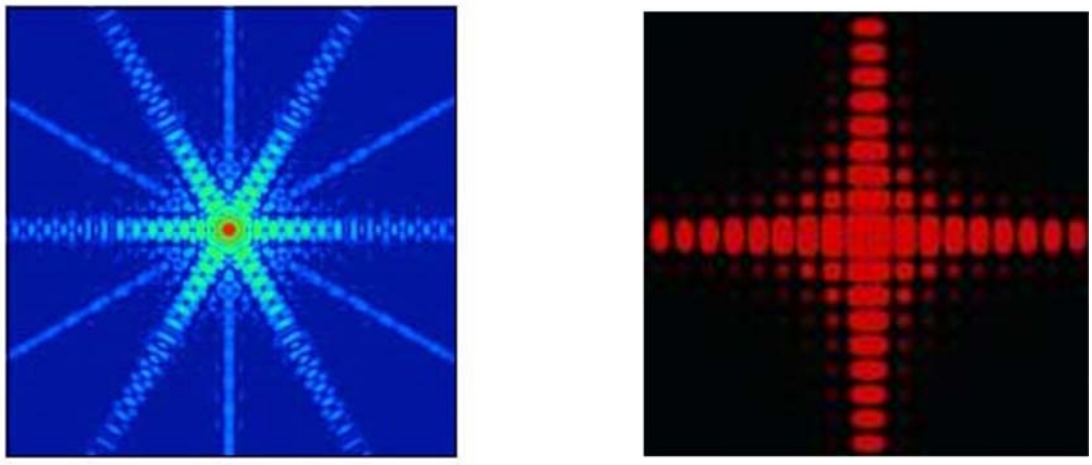

Figure 1. Point spread functions of a hexagonal (left panel) and a square (right panel) aperture, both on logarithmic scales. The spokes are results of diffraction off the aperture edges. Having many such segments increases the contrast even more.

structure, and avoids light contamination between the gaps. The straight edges of these elements share common orientations, which scatter a great deal of light in the focal plane of the telescope. This scattered light appears as coherent spokes, which limit the ability to detect faint objects next to a bright one (Figure 1). Pushing all the scattered energy in a few directions can be useful for planet search (and led to the discovery of Sirius B in 1909). However, it does not improve the quality of general images.

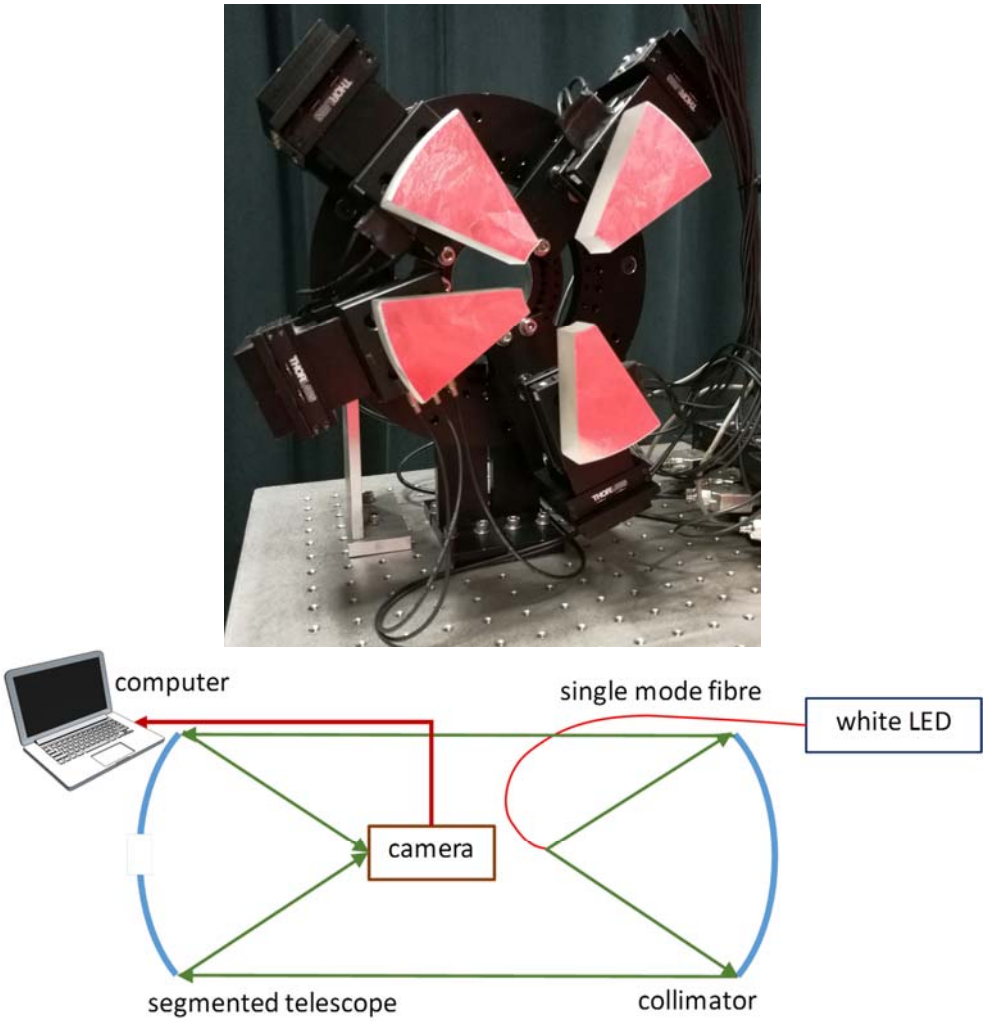

Figure 2. Laboratory experiment. Top: A 200 mm segmented sparse telescope (surface reflection from pink packaging material). The segments were cut from a full parabola, each was a 30^0 sector, with a central bore of 50 mm. Each segment has three degrees of freedom, essentially tip, tilt and piston. Bottom: Experimental set up. A single-mode fibre is being fed by a white LED, and is placed at the focus of the collimator. Light from the collimator is reflected back into the segmented parabola prime focus, where a high-pixel count camera is placed. The segments actuators are controlled by the central computer.

In the laboratory model that we have built (Figure 2) this is very clear. This model is very simple: two parabolas facing each other, the first a collimator, the second the segmented telescope model. White light is inserted in the prime focus of the collimator, and a camera is placed at the focus of the telescope. Analysis of the camera images leads to computerised commands to the sectors PZT actuators. It is very easy to see that the straight edges of the segments, sawn from a full parabola, diffract a great deal of light normal to their directions (Figure 3). For reduced redundancy, they were oriented at different angles (see below).

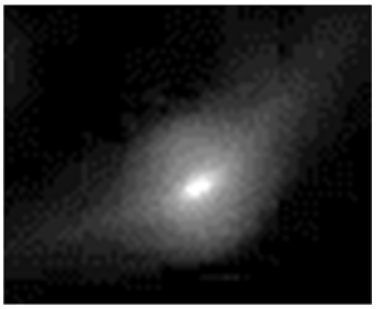

Figure 3. The focal image of one of the segments in Figure 2, highly magnified (linear scale). Notice the two long spokes stretching from the centre of the image, and the two broad ones at the other directions.

2. **Options**

One solution for reduction of these artifacts is to round the edges of the sub-apertures. This is because the borders of the aperture scatter light by diffraction, and the shortest edges (compared to the area) can be found in circular apertures. While fully circular segments are easiest to implement, they enlarge the volume of the stowed telescope. Elliptical segments [7] are a viable option: they have no straight edge, they are easy to stow and deploy, and are straightforward to manufacture. Indeed, their PSF has the same central spike as when using the hexagonal segments. However, the off-axis focal plane energy is not oriented into specific directions. Rather, it is diffracted quite evenly in all orientations (Figure 4). The rounded shapes of the segments make also for a smoother mutual transfer function (Figure 5).

3. **Removing redundancy 1**

As we see in Figure 3, each sector has its own unique PSF, and two sectors at different angles can be differentiated by their orientation. We used four matched filters the four PSF angles, and used the estimated centres of the correlations to correct for their tip and tilt. Notice that another method tilts the segments one after the other out of and back into the field of view for their identification. Additionally, if the PSFs overlap at the focal plane, the telescope is defocused to separate them and the process is repeated.

In a manner similar to that of the sectors, we simulated four equal elliptical segments inscribed inside a circular aperture in a Cassegrain or prime focus configuration. We were able to uniquely identify each one by its rotation about the center.

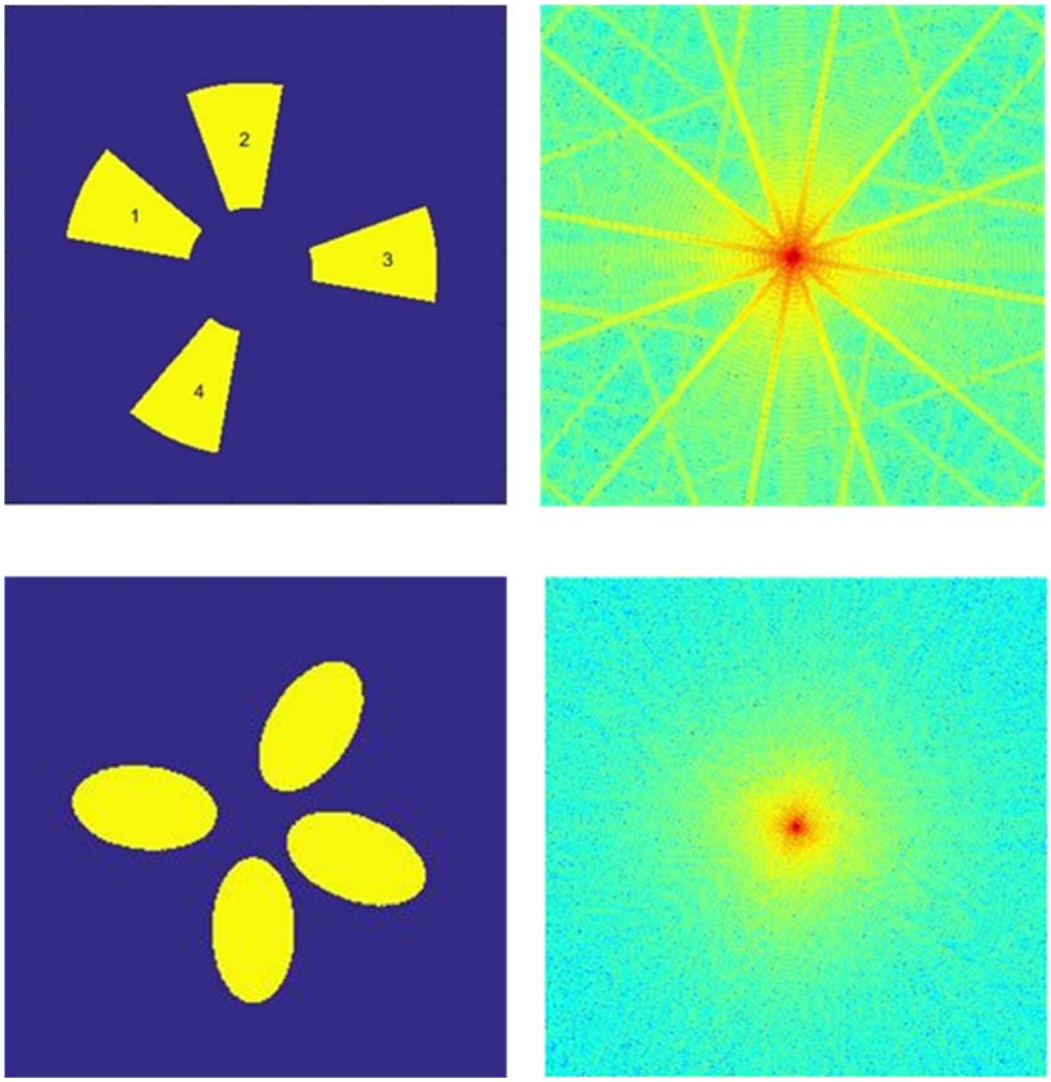

Figure 4. Modeled and calculated segments (left) and their point spread function (right, log scale): sectors (top) and ellipses (bottom). Notice that the spokes, so evident in the sectors PSF, have averaged out in the ellipses PSF. In addition, since the relative lengths of the perimeters of the ellipses are shorter than those of the corresponding sectors, less light is being scattered from them.

4. **Removing redundancy 2**

Another benefit of the rotated segments is their auto-correlation in the *uv* plane, shown in Figure 5. Here each pair of segments was optimized to occupy a unique area (compare the top-left panels of Figures 4 and 5). The phases of the fringes between these ellipses appear in these common areas and enable the measurement of their optical path differences [8].

We optimised the axes ratio *a*/*b* of the segments as one free parameter, and their angular separations around the telescope aperture as three more parameters (the fourth separation is not a free parameter, they have to add up to 360^0). The target criterion was either to obtain the

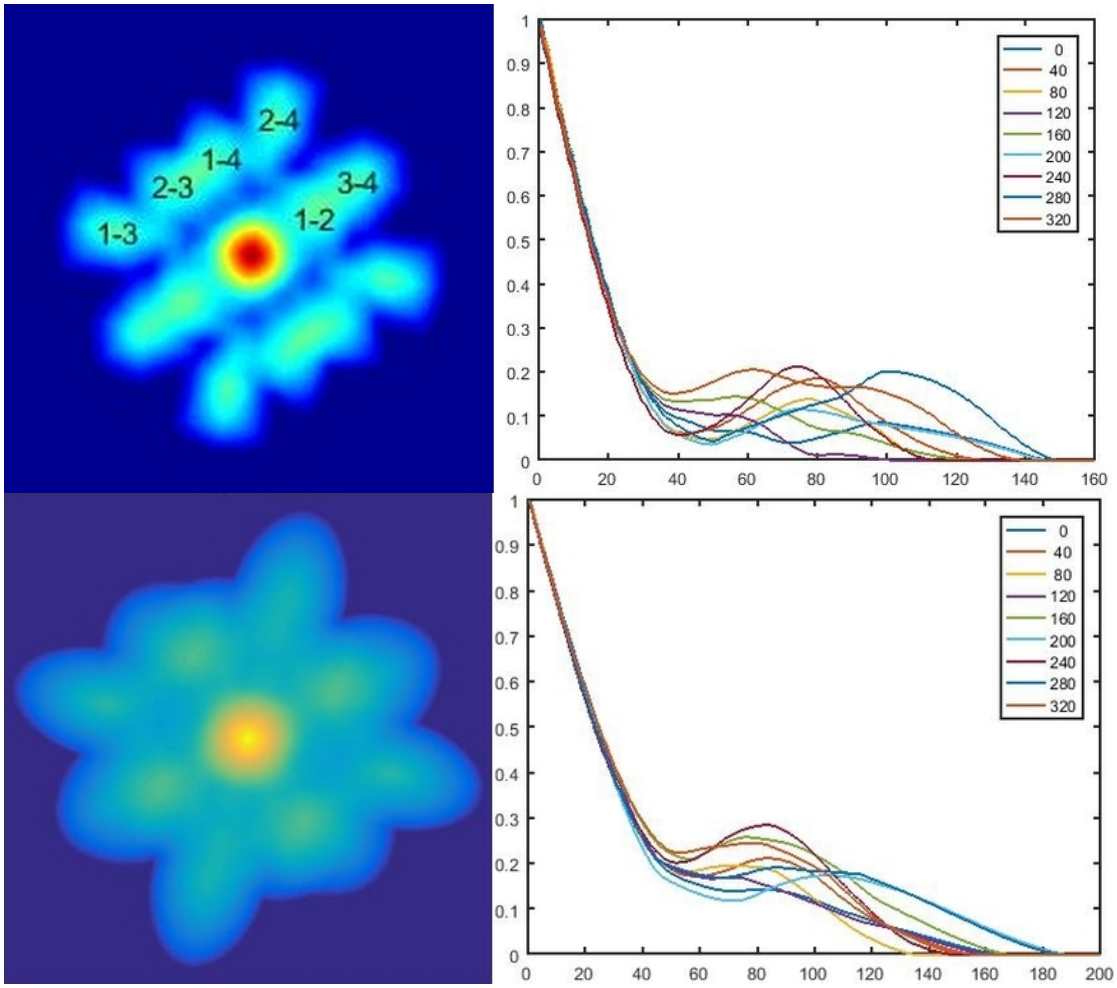

Figure 5. Left panels: The mutual transfer function (the Fourier amplitude of the PSF, or the aperture auto-correlation function) of the elliptical sectors. The MTF of the ellipses (bottom) can now be optimised to be smoother than that of the straight-edge sectors (corresponding rows in Figure 4). The lobe numbers correspond to the panel numbers in Figure 4. Right panels: Cuts of the MTF along different orientations, at 30^0 steps. Notice that the MTF curves are smoother with rounded panels (bottom right).

widest MTF, or to maximise the MTF smoothness. Solutions that had regions in the MTF that were below a threshold were rejected: in image reconstruction, division by such MTFs would be difficult to regularise. Of course, solutions with flipped or rotated configurations were considered the same. After thousands of optimisations, the results for the two criteria, smoothest or widest MTF, were very similar (Figure 5). For the axes ratio *a*/*b* of 1.5 to 2.2 that we tested, the azimuthal angles between segments were 66.8±3.4, 83.8±5.2, 113.0±4.5 and 96.4±6.3 degrees.

5. **Conclusions**

While today aperture masking and segmented telescopes have a symmetrical design for the sub-apertures shapes, we advocate here breaking that symmetry. While more challenging to plan and research, the mechanical advantage for non-standard shapes is minimal. The polishing requirements are very similar - off axis parabolas, in most parts. The machining of the edges is quite similar for straight or rounded segments. These manufacturing issues are not relevant at all for aperture masking.

There are no hard rules here. For example, in our case, we looked at the option of four segments, as in the laboratory model, and optimised their orientations, not Cartesian placements. Thus the apertures should be designed for each system according to its constraints, but with added care to minimising the perimeter-to-area ratio for less scattered light, and for more flexibility in aperture placement.

Support for this project was provided in parts by the Israeli Ministry of Science

References

[1] R A Muller and A Buffington, Real-time correction of atmospherically degraded telescope images through image sharpening. *JOSA* **64,** 1200-10 (1974)
[2] J P Hamaker, J D O'Sullivan, and J E Noordam, Image sharpness, Fourier optics, and redundant-spacing interferometry, *J. Opt. Soc. Am.* **67**, 1122-3 (1977).
[3] M J Booth, D Débarre, and T Wilson, Image-based wavefront sensorless adaptive optics. *Advanced Wavefront Control: Methods, Devices, and Applications V*, *SPIE* **6711**, 671102 (2007)
[4] N Brosch, V Balabanov and E Behar, Ultraviolet astronomy with small space. *Astrophysics and Space Science* **354,** 205-9 (2014)
[5] M. J. Golay, Point arrays having compact, nonredundant autocorrelations. J. Opt. Soc. Am. 64, 272-273 (1971)
[6] D Dolkens, G Van Marrewijk and H Kuiper, Active correction system of a deployable telescope for Earth observation. *SPIE* **11180**, 111800A (2019)
[7] E N Ribak and S Gladysz, Fainter and closer: finding planets by symmetry breaking, Optics Express 16, 15553 (2008)
[8] E N Ribak, B M Levine, Phasing a sparse telescope, This meeting, paper SPIE 11443-182 (2020)